RESEARCH ARTICLE | OCTOBER 06 2023

Effect of NaOH treatment on rice husk-derived graphene on the presence of crystalline silica

Adinandra Caesar Fachrudin ✉; Evvy Kartini; Muhammad Fakhrudin; Alan J. Drew

AIP Conf. Proc. 2932, 020004 (2023)
https://doi.org/10.1063/5.0174828

Effect of NaOH Treatment on Rice Husk-Derived Graphene on the Presence of Crystalline Silica

Adinandra Caesar Fachrudin[1, a)], Evvy Kartini[1, 2, b)], Muhammad Fakhrudin[1, 2] and Alan J. Drew[1, 3]

[1] *National Battery Research Institute, Indonesian Life Science Center, Technology Business Zone BRIN Puspiptek Area, Bogor, 16340, West Java, Indonesia*
[2]*Research Center for Advanced Material, Research Organization for Nanotechnology and Materials, National Research and Innovation Agency, Puspiptek Area, South Tangerang, Banten 15314, Indonesia*
[3] *School of Chemical and Physical Sciences, Queen Mary University of London, 327 Mile End Road, London E1 4NS, United Kingdom, UK*

a) Corresponding author: adinandra12caesar@gmail.com
b) evvy.kartini@n-bri.org

Abstract. Graphene is produced using green synthesis approaches from rice husk, called rice husk-derived graphene (GRHA). Due to the high silicon content compared to carbon in raw rice husks, this research will add sodium hydroxide (NaOH) treatment to reduce silica in the resulting GRHA, commonly known as desilication. Rice husk ash (RHA) was mixed with NaOH solution by stirring at 80 °C for 3 hours, followed by filtering, washing, and drying. Variation in NaOH concentration is 0.5, 1.0, and 1.5 M to study the optimal one added between the carbonization and activation at high temperature with potassium hydroxide (KOH). EDS spectra confirmed that the NaOH treatment could reduce silica, and the most optimal concentration was found at GRHA-1.0, as it possessed the highest carbon content of up to 80.27%. SEM images also showed a crumpled structure of layered graphene with a thickness of several nanometers. XRD patterns showed that the three samples still contain silica with a high degree of crystallinity. It is due to the thermal treatment, which is also responsible for converting silica from amorphous to crystalline. This methodology is a promising way to increase the added value of rice husks with a cost-effective process while reducing the wasted as an environmental burden.

INTRODUCTION

Rice husk (or rice hull) is a hard protective covering of rice grains and a by-product of the rice milling process in the agro-based industry. So, it is one of the most widely available agricultural wastes in many rice-producing countries worldwide, especially in Indonesia. According to the Food and Agriculture Organization (FAO), Indonesia is the fourth top rice-producing country after China, India, and Bangladesh, with a total production of 54 million tonnes of rice in 2020. Moreover, rice is the third most produced crop worldwide, contributing 8% of global primary crop production behind sugarcane (20%) and maize (12%) in the same year. However, due to its low economic value and difficulty in decomposing, most rice husk is either burnt or dumped after being cultivated and harvested, resulting in abundant availability and fast-growing characteristics [1]. It causes pollution that can ultimately harm the health of many organisms, including humans, and affect the quality of the environment, both land and air. Therefore, apart from being a crucial task, research on agricultural waste management as a natural resource material is a state-of-the-art and desirable subject in the fields of science and engineering [2].

As biomass, rice husk contains organic and inorganic compounds, which vary depending on the origin and the process involved in its growth. Generally, the main constituent of rice husk comprises around 70 – 80% organic matter consisting of cellulose, hemicellulose, and lignin. The latter is more complex and dominant than the other two, as it holds the most carbon linkage of the lignocellulosic components [3]. Rice husk is also composed of about

The International Conference on Battery for Renewable Energy and Electric Vehicles (ICB-REV) 2022
AIP Conf. Proc. 2932, 020004-1–020004-10; https://doi.org/10.1063/5.0174828
Published by AIP Publishing. 978-0-7354-4692-2/$30.00

20 – 30% inorganic residues, mainly silica, and small amounts of impurities from dust and metals. It opens up vast opportunities to turn waste into beneficial applications safely and sustainably. Initially, rice husk is mainly used as a raw material for ceramic or an admixture for cement, as the amorphous silica extraction is pretty straightforward [2,4–6]. Lately, along with sophisticated technology development, rice husk is also successfully synthesized into various carbon derivatives ranging from activated carbon [7] to carbon quantum dots [8] and silicon/carbon [9]. Among these materials, one that grabs much attention is its conversion into graphene. Up to now, previous research and studies have shown promising potential to produce high-quality graphene, eventually.

Graphene, a carbon allotrope consisting of a two-dimensional honeycomb crystal lattice structure of single-layered atoms bonded by sp^2 hybridization, has received extensive research attention in the last 2-3 decades for its multidisciplinary applications [10]. Graphene has many outstanding properties, such as being extremely strong and elastic, possessing superior surface area and optical transparency, exhibiting excellent thermal and electronic conductivity, and its biocompatibility for medical uses [11]. There are two main approaches for synthesizing graphene: top-down, such as chemical reduction [12], mechanical exfoliation [13], and arc discharge [14], and bottom-up, such as chemical vapor deposition [15], and epitaxial growth [16]. However, the synthesis route mentioned above is relatively expensive and complicated. Recently, researchers have suggested and developed a green synthesis approach for producing graphene using environmentally-friendly carbon sources [17]. The main objective is to utilize less toxic chemicals and more natural precursors. One of this approach's significant challenges is to optimize the parameters and methods and control the size, quality, and morphology, as well as commercial investigations for scale-up production [18]. Nonetheless, rice husk utilization into graphene, called rice husk-derived graphene (GRHA), will increase the added value of rice husk and decrease the production cost of graphene.

Muramatsu's group first reported graphene from rice husk ash (RHA), solid rice husk residue, using potassium hydroxide (KOH) as an activation agent at 850 °C. The result, called rice husk-derived graphene (GRHA), consists of nano-sized crystalline graphene and corrugated graphene with atomically smooth surfaces and edges [17]. Later, some improvements used rice husk as not only a graphene precursor but also a protective barrier against oxidation, which previously used carbon black [19]. Generally, the GRHA synthesis consists of carbonization, in which rice husk was in air combustion to get RHA, and activation processes. Several factors contribute to the quality and characteristics of the resulting GRHA, such as pre-treatment temperature, RHA and KOH ratio, activation time, and after-treatment (e.g., sonication, exfoliation, etc.). When rice husk is at high-temperature carbonization (550 – 700 °C), it shows a significant change in the pore structure resulting in a different surface area; the lower the temperature, the higher the surface area [20]. The surface area is closely related to the adsorption performance of the material and sometimes indicates better quality of graphene. In addition, other researchers tried to use a lower carbonization temperature (100 – 400 °C) to make it more cost-effective. They found the optimal one at 200 °C, as it possessed wrinkled structures and a few layers of graphene flakes that lead to the highest surface area [21].

The ratio between RHA and KOH is crucial in determining the amount and structure of the resulting GRHA. Increasing the amount of activation agent (from 1:2 and 1:4 to 1:5) seems to increase the relative amount of graphene content and improve the porosity of the formed surface structure [22,23]. Along with the numerous success of GRHA synthesis, researchers have begun to show its potential applications in various energy storage [24–26]. This utilization of rice husk will pave the way for sustainable production of energy storage. Due to the presence of silica, as the most residue in the ash, Seitzhanova's group started to add desilication between these two processes with sodium hydroxide (NaOH) by simply mixing [27]. However, the result was unclear, as it was not explained the influence of desilication on the whole synthesis process. Therefore, this research aims to study the effect of NaOH treatment by varying its concentration compared to without desilication. The methodology showed a significant difference in silica's elemental composition and phase transformation. Furthermore, comparative analysis with other literature is also discussed to explain this phenomenon.

METHODOLOGY

Material

Rice husk was used as a starting material, along with glass wool as a cover for the material to prevent oxidation. Sodium hydroxide (NaOH) and potassium hydroxide (KOH) obtained from Merck were used as desilication and activation agents, respectively. Graphene obtained from Shandong Yuhuang was also used to compare the resulting GRHA. All pure analytical materials were used without any further purification.

Synthesis

The methodology includes carbonization, desilication, and activation. Carbonization aims to obtain carbon. The rice husk was washed with deionized (DI) water to remove impurities and dried in the oven at 110 °C overnight. After that, the rice husk was compacted into a ceramic crucible and heated in the furnace at 200 °C for 10 hours to get rice husk ash (RHA). Then, the RHA will go into desilication that aims to remove silica. The RHA mixed in NaOH solution with a ratio of 50 mL of solution per gram of RHA varied at concentrations of 0.5, 1.0, and 1.5 M. The mixed solution was heated at 80 °C under constant magnetic stirring at 350 rpm for 3 hours, followed by decantation and filtration. The resulting sample was washed with DI water several times to reach the equilibrium of pH around 7.0 and dried in the oven at 110 °C for 2 hours.

The final step is activation, which aims to form graphene. RHA and KOH in a ratio of 1:5 were mixed until homogeneous conditions. Due to the difficulty of crushing KOH pellets through grinding, the mixing is achieved by dissolving KOH in a minimum of water. Then, add the RHA and evaporate the remaining water until the mixture is dried. The mixture was compacted into an alumina crucible and then placed in the midpoint of a giant alumina crucible, filled with glass wool and rice husk in the space between the two crucibles, and covered with a crucible cap to prevent oxidation against air. Then, the mixture was annealed in the furnace at 850°C using a heating rate of 5 °C/min for 2 hours in a nitrogen atmosphere. Same as before, the resulting sample was washed with DI water several times to reach the equilibrium of pH around 7.0 and dried in the oven at 110°C for 2 hours.

Characterization

The samples were denoted as GRHA-x, where x is NaOH concentration in the desilication process. Morphological features were studied using a scanning electron microscope-energy dispersive X-ray spectroscopy (SEM-EDS) (JSM-6510LA, Jeol Ltd.) with an energy range of 0 - 20 keV at a voltage of 10 kV. Crystal structures were checked by X-ray diffraction (XRD) (PIXcel1D, Malvern Panalytical) using a copper X-rays spectrum with an angle range of 5° - 80° at a step of 0.02626°. Both characterization methods were performed on the RHA, GRHA, and commercial graphene.

RESULTS AND DISCUSSION

The conversion of rice husk into graphene through a green synthesis approach consists of three-step, including activation, desilication with NaOH, and activation with KOH. The brown precursor will change into black ash after carbonization. Initially, RHA did not undergo much change from the rice husk form, only it was more brittle, which then went through mechanical crushing to make it into ash and some into gas. The NaOH treatment of RHA for desilication also helps to crush RHA further, becoming like a brittle flake. Before activation, RHA and KOH were mixed until homogeneous conditions, resulting in a dough-like mixture. Annealing at a very high temperature will then completely change the form and structure of the material to produce GRHA. After some washing and drying, the product yield will finally be a mixture of grey-like and black powder.

The visual appearance of samples showed that desilication makes the resulting GRHA darker. It is assumed to indicate element composition changes in the materials, as carbon-based materials tend to be black while silicon-based materials are white. However, It can also show impurities due to the influence of other atoms such as potassium, natrium, and aluminium from the agents and crucible. In addition, desilication also makes the resulting GRHA lighter. Although the mass of pure GRHA material is more, the amount of powder from GRHA material with desilication looks much more. There is an exception in GRHA-1.5; it remains black, but the amount of powder looks less than GRHA-0.5 and GRHA-1.0, which is an early indication of the turning point of NaOH treatment.

All samples were weighed in every process to compare the mass loss and product yield. Table 1 shows that the mass loss in each process continues to increase, resulting in a small product yield. The mass loss during desilication at various NaOH concentrations was not much different, around 56%, but during activation, there was a significant change compared to pure GRHA material. The higher the concentration, the greater the mass loss. Figure 1 shows that the best product yield achieved is only about 10%. Although GRHA-0.5 material has less mass loss during activation, its product yield differs slightly from pure GRHA material. It indicates that the effect of NaOH treatment changes the properties and structure of the material, in which high concentration makes the material less dense so that it is easier to decompose, resulting in the formation of more gas phases during activation. Up to this point, the results show that a lower concentration will be better in producing more product yield.

TABLE 1. The mass loss of each process compared to the previous step.

Sample	Carbonization	Desilication	Activation
GRHA	43.43%	-	83.18%
GRHA-0.5	43.43%	55.36%	63.34%
GRHA-1.0	43.43%	56.09%	82.77%
GRHA-1.5	43.43%	56.63%	92.71%

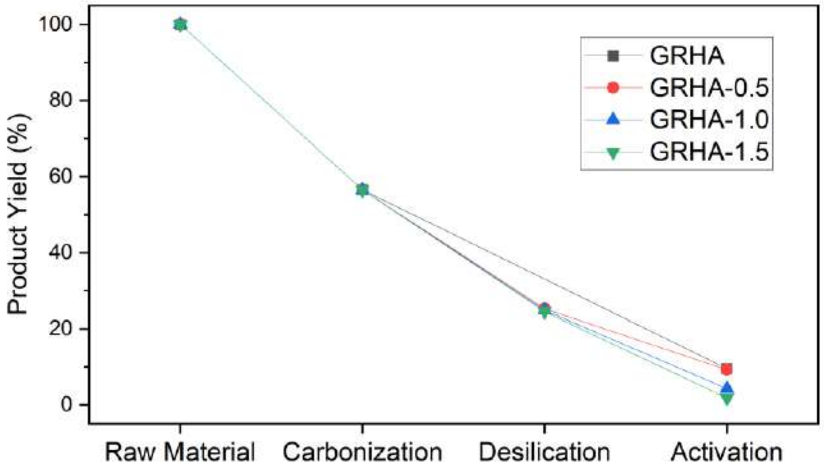

FIGURE 1. The product yield of each process compared to the initial rice husk mass.

The product yields of GRHA, and GRHA-1.0 are 9.51% and 4.28%, confirming similar results to pure GRHA from [17] of about 10% and GRHA with 1.0 M NaOH concentration for desilication from [27] of about 3%. Other researchers showed better product yields of up to 20 – 30% by changing activation conditions in vacuum environments to slow the oxidation rate [19,20]. Generally, biomass or natural precursor contain only relatively low product yields, which is a primary consideration of economic value and inefficient process [3,28]. In the case of graphene, other elements, such as oxygen and nitrogen, are worthy of investigation, as they also significantly influence product yields. But apart from that, this effort is crucial to reduce and utilize abundant waste. One of the main ways of enhancing product yields is through acid treatment [25,29,30]. It is due to its ability to modify and promote the lignocellulosic matrix [31,32].

Figure 2 shows morphological features of graphene, RHA, and all GRHA samples from SEM-EDS results. RHA depicted irregular morphology without any crumpled or wrinkled structure and showed smooth surfaces with non-porous shapes, as shown in Fig. 2b. EDS spectrum also showed that RHA has content more dominant in silicon than carbon. However, its morphology cannot describe the differences in the constituent atoms since they were still in amorphous forms. After undergoing activation with KOH, GRHA showed a crumpled structure of layered graphene, as shown in Fig. 2c, which looked relatively thicker than GRHA-x. KOH-treated demonstrated removal of amorphous form efficiently. However, it was entirely different from the morphology of commercial graphene in Fig 2a, which showed a flake structure with rough surfaces ranging in size from 5 to 50 µm. It is noteworthy that graphene has various morphologies that depend on the synthesis method with their respective advantages. This crumpled structure will support a higher surface area, especially for energy storage applications [33].

NaOH-treated samples clearly showed the presence of silica particles, which were agglomerated and scattered along layered graphene, as shown in Figs. 2d, 2e, and 2f for GRHA-0.5, GRHA-1.0, and GRHA-1.5, respectively. When comparing the three samples, it can be ascertained that GRHA-1.0 appeared as the most desirable morphology, had generally larger graphene layers compared to GRHA-0.5 and GRHA-1.5, but contained almost no silica particles showing only a smooth layer with a thickness of several nanometers. It is assumed that the presence of silica particles could break graphene layers into smaller ones. It is possible to diminish the quality and deteriorate the performance of graphene due to the increasing number of defects. These defects are sometimes beneficial for manipulating their thermal, electronic, and mechanical behavior [34–36]. However, in order to compare the properties of graphene in general, fewer defects are preferable. In short, these results are similar to those shown by some other researchers [19,24,26,27].

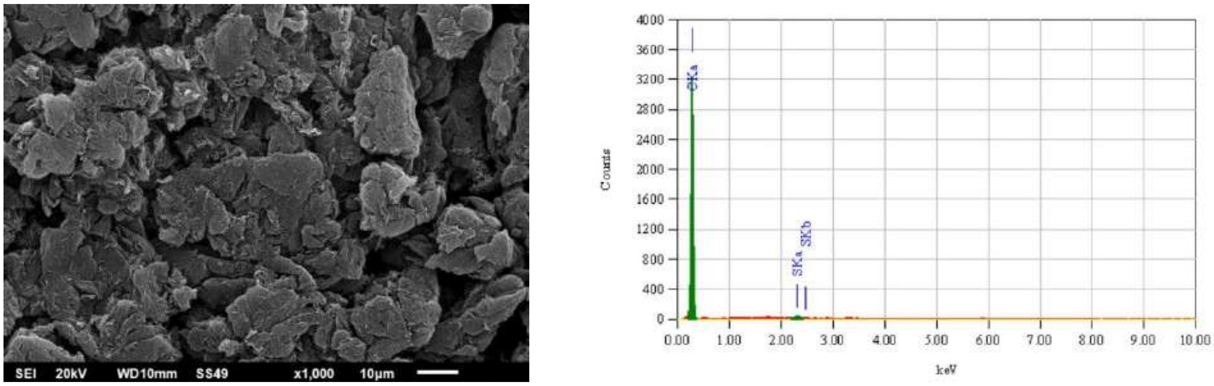
SEI 20kV WD10mm SS49 x1,000 10μm
CKa
SKa
SKb
Counts
keV
0.00 1.00 2.00 3.00 4.00 5.00 6.00 7.00 8.00 9.00 10.00
0 400 800 1200 1600 2000 2400 2800 3200 3600 4000

(a)

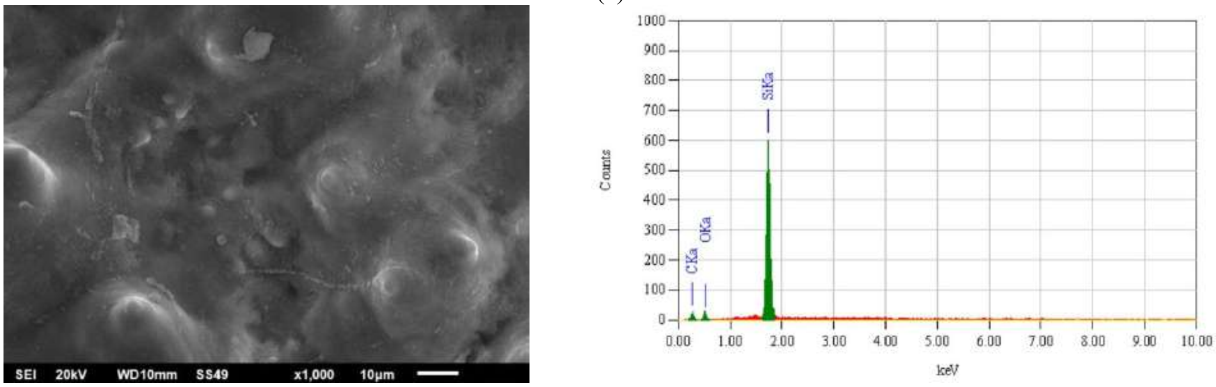
SEI 20kV WD10mm SS49 x1,000 10μm
SiKa
CKa
OKa
Counts
keV
0.00 1.00 2.00 3.00 4.00 5.00 6.00 7.00 8.00 9.00 10.00
0 100 200 300 400 500 600 700 800 900 1000

(b)

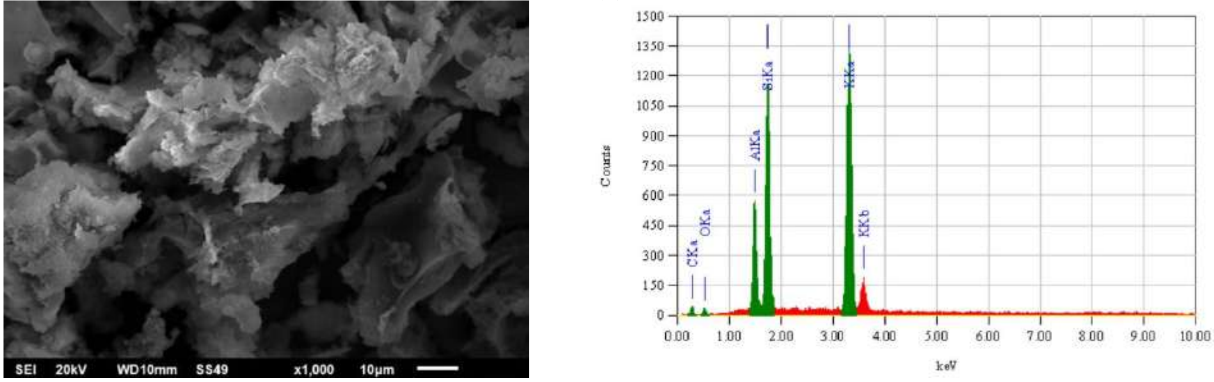
SEI 20kV WD10mm SS49 x1,000 10μm
SiKa
KKa
AlKa
CKa
OKa
KKb
Counts
keV
0.00 1.00 2.00 3.00 4.00 5.00 6.00 7.00 8.00 9.00 10.00
0 150 300 450 600 750 900 1050 1200 1350 1500

(c)

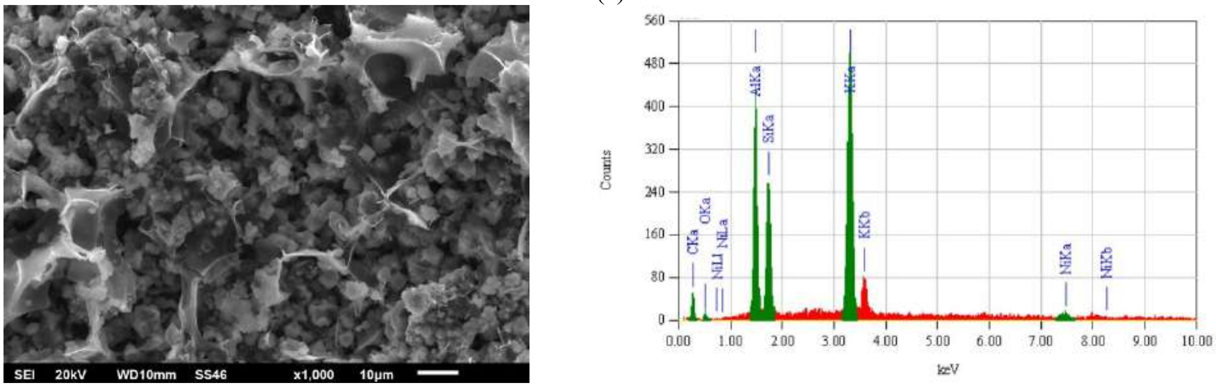
SEI 20kV WD10mm SS46 x1,000 10μm
AlKa
KKa
SiKa
CKa
OKa
NiLl
NiLa
KKb
NiKa
NiKb
Counts
keV
0.00 1.00 2.00 3.00 4.00 5.00 6.00 7.00 8.00 9.00 10.00
0 80 160 240 320 400 480 560

(d)

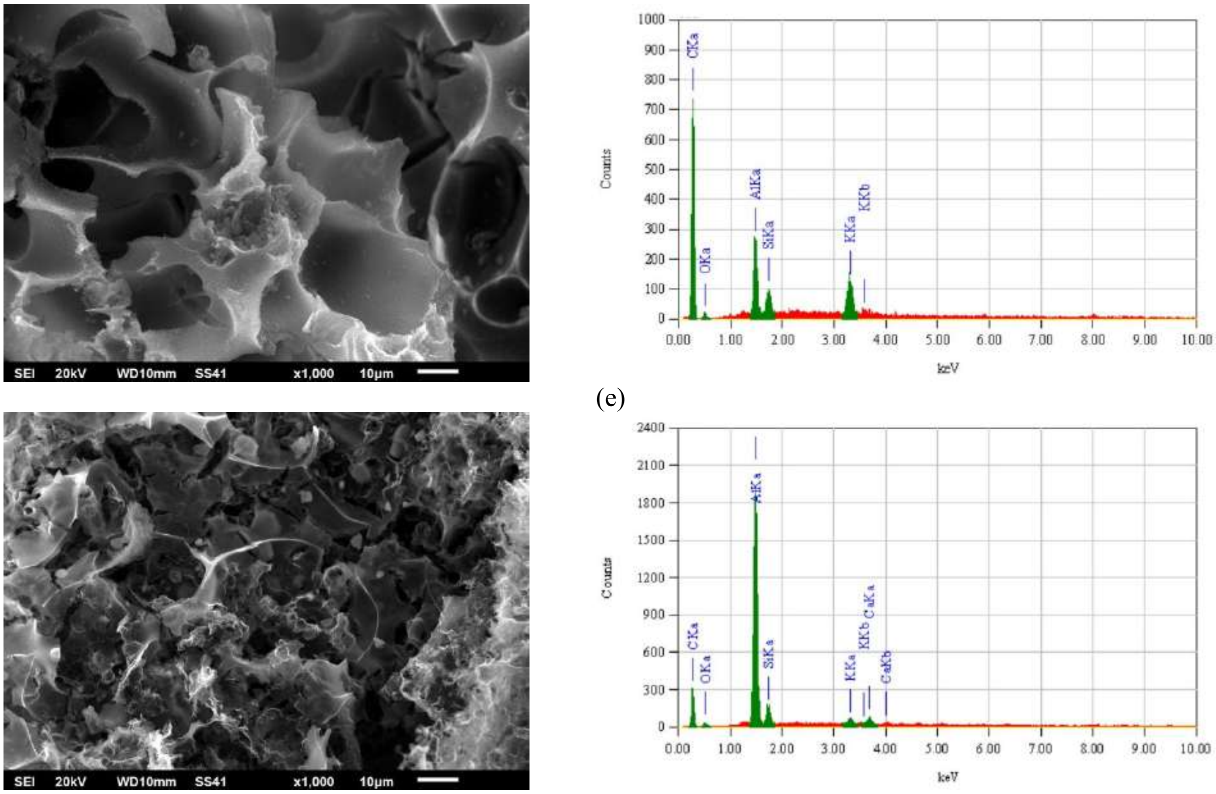

FIGURE 2. SEM images (left) and EDS spectra (right) of (a) Graphene, (b) RHA, (c) GRHA, (d) GRHA-0.5, (e) GRHA-1.0, and (f) GRHA-1.5.

EDS spectra described elemental analysis of both peaks and percentages. Tables 2 and 3 show the elemental composition of graphene, RHA, and all GRHA samples by their mass and atom, respectively. Despite still having more dominant content in silicon than carbon in GRHA, these results obviously demonstrated NaOH treatment's effectiveness at different concentrations in removing silica. Compared to initial RHA content, the silicon mass reductions of GRHA, GRHA-0.5, GRHA-1.0, and GRHA-1.5 are 43.05%, 69.05%, 95.11%, and 92.34%, respectively. These reductions by the atom only have slightly different. It supported morphological analysis in the previous paragraph and confirmed that KOH-treated could help remove silica, which also has the critical function of inducing surface porosity and enriching edge structure [3,37]. It is assumed that there is an indication of linearity between increasing NaOH concentration and reducing silicon content, although there is a slight downtrend in GRHA-1.5. Several aspects determine the relatively low carbon content in this research except for GRHA-1.0: (i) different raw materials which had typically small carbon sources; (ii) synthesis environments using a non-vacuum furnace which makes the oxidation rate still quite high; and (iii) large impurities of entrapped potassium from activation agent and aluminum from alumina crucible. Therefore, GRHA-1.0 seems the most optimal, exhibiting the highest carbon content of up to 80.27% and the least impurities of only 12.29%.

TABLE 2. Element composition by the mass of all samples from EDS spectra.

Sample	**Element Composition by Mass (%)**							
	C	**Si**	**O**	**S**	**K**	**Al**	**Ni**	**Ca**
Graphene	99.31	-	-	0.69	-	-	-	-
RHA	38.08	45.81	16.12	-	-	-	-	-
GRHA	9.44	26.09	8.25	-	44.83	11.40	-	-
GRHA-0.5	23.25	13.97	6.68	-	33.92	18.94	3.24	-
GRHA-1.0	80.27	2.24	5.21	-	4.83	7.46	-	-
GRHA-1.5	57.81	3.51	4.72	-	1.35	31.01	-	1.60

TABLE 3. Element composition by the atom of all samples from EDS spectra.

Sample	Element Composition by Atom (%)							
	C	**Si**	**O**	**S**	**K**	**Al**	**Ni**	**Ca**
Graphene	99.74	-	-	0.26	-	-	-	-
RHA	54.58	28.08	17.34	-	-	-	-	-
GRHA	20.68	24.45	13.57	-	30.18	11.12	-	-
GRHA-0.5	43.26	11.11	9.33	-	19.38	15.69	1.23	-
GRHA-1.0	89.25	1.06	4.35	-	1.65	3.69	-	-
GRHA-1.5	74.55	1.94	4.56	-	0.53	17.80	-	0.62

Crystal analysis is determined from the XRD patterns of all samples, as shown in Figure 3. It is also essential for identifying its phase transformation with and without desilication. A subtract baseline was firstly performed using Origin software to compare the diffraction peaks more clearly. The presence of graphene in GRHA and GRHA-x was confirmed at diffraction peaks around 29° and 43°, corresponding to the (002) and (100) lattice planes of carbon, respectively. Different from that reported by Muramatsu's group, NaOH-treated samples show a dominant and intense (002) peak, specifying the presence of a regularly stacked graphitic structure due to the breakage of the interplanar C-bonds in the growth of graphene [17]. It also confirmed the effect of carbonization temperature at 200°C, in which this peak will weaken or even disappear at higher or lower temperatures [21]. On the other hand, the (100) peak indicated the formation of pore structure along the direction of a graphitic structure, rising a relatively well-organized aromatic carbon that is more stable than amorphous carbon [37]. Therefore, it is assumed that NaOH-treated samples exhibit a higher surface area and multilayer graphene due to a consistent increase in the peak intensity. However, this research was not able to assure these two characteristics in the absence of characterization from Raman spectroscopy and Brunauer-Emmett-Teller (BET).

Compared to a broad single carbon peak in commercial graphene, GRHA showed relatively narrow diffraction peaks indicating the predominant crystalline forms. The disappearance of a wide and high silica peak around 23° from the XRD pattern of RHA initially indicated the primary silica removal from KOH treatment. However, one of the most observed is that GRHA-x samples generally presented more diffraction peaks than pure GRHA. These additional peaks were confirmed by Sharma's group, which reported it corresponds to cristobalite silica [38]. But it didn't rule out the influence of other minerals, such as quartz, coesite, zeolite, cristobalite, etc. It turned out that the NaOH treatment used in this research led to phase transformation with a high degree of crystallinity from amorphous forms in RHA. Although the thermal treatment is also responsible for the occurrence of this phase transformation, it is somehow not significantly affected when without desilication. Conversion of remaining silica into crystalline form, which was not expected to occur, is not conducive to successfully reducing silicon content by the NaOH treatment. Hence, it needs further comprehensive understanding and more scientific explanation to bridge the knowledge about this phenomenon. However, comparing those three samples will be consistent with the results that GRHA-1.0 showed the most favorable, as it has peaks correlated to silica lower than the other NaOH-treated samples. Moreover, a combination of all analyses concluded that the most optimal NaOH concentration was still 1.0 M.

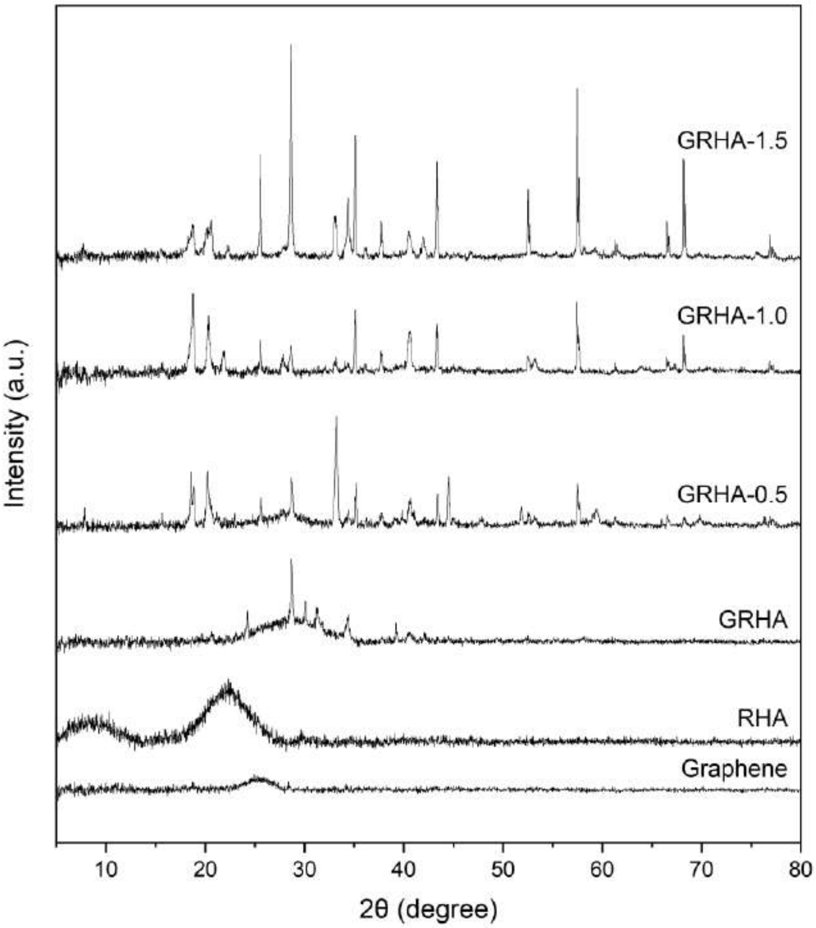

FIGURE 3. XRD patterns of Graphene, RHA, and all GRHA samples.

CONCLUSION

Graphene is produced successfully using a three-step green synthesis approach from rice husk by adding desilication with NaOH between the two primary methods. Variations in the NaOH concentration from 0.5 to 1.0 and 1.5 M significantly differed in silica's elemental composition and phase transformation. The findings and analysis of the present research suggest 1.0 M as the most optimal NaOH concentration, as GRHA-1.0 possessed the highest carbon content of up to 80.27% and reduced the silicon content by 95.11%. It showed a crumpled structure of layered graphene with a smooth layer and a thickness of several nanometers. NaOH treatment tends to make the resulting GRHA darker and lighter, but the higher the concentration, the greater the mass loss and the lower the product yield. It also converted the remaining silica from amorphous to crystalline. However, further understanding and explanation of these crystal peaks still need more in-depth study. The results provide insights into desilication with NaOH for reducing silica to obtain a better quality of GRHA and encourage the utilization of rice husk into high-value-added material for reducing waste through a cost-effective process. Further research is necessary for using different concentrations, applying other desilication agents, and optimizing existing methods for reducing the remaining impurities.

ACKNOWLEDGEMENT

This work is fully financially supported by the National Battery Research Institute (NBRI).

REFERENCES

1. S. Steven, E. Restiawaty, and Y. Bindar, Renewable and Sustainable Energy Reviews **149**, 111329 (2021).
2. H. Moayedi, B. Aghel, M.M. Abdullahi, H. Nguyen, and A. Safuan A Rashid, Journal of Cleaner Production **237**, 117851 (2019).
3. M.T. Safian, U.S. Haron, and M.N. Mohamad Ibrahim, BioResources **15**, 9756 (2020).
4. S.S. Hossain, L. Mathur, and P.K. Roy, Journal of Asian Ceramic Societies **6**, 299 (2018).
5. W.H. Kwan and Y.S. Wong, Materials Science for Energy Technologies **3**, 501 (2020).
6. M. Amran, R. Fediuk, G. Murali, N. Vatin, M. Karelina, T. Ozbakkaloglu, R.S. Krishna, A.K. Sahoo, S.K. Das, and J. Mishra, Crystals (Basel) **11**, 168 (2021).
7. S. He, G. Chen, H. Xiao, G. Shi, C. Ruan, Y. Ma, H. Dai, B. Yuan, X. Chen, and X. Yang, Journal of Colloid and Interface Science **582**, 90 (2021).
8. N.H. Zainal Abidin, V. Wongso, K.C. Hui, K. Cho, N.S. Sambudi, W.L. Ang, and B. Saad, Journal of Water Process Engineering **38**, 101634 (2020).
9. H. Chu, Q. Wu, and J. Huang, Colloids and Surfaces A: Physicochemical and Engineering Aspects **558**, 495 (2018).
10. S.K. Tiwari, S. Sahoo, N. Wang, and A. Huczko, Journal of Science: Advanced Materials and Devices **5**, 10 (2020).
11. F. Farjadian, S. Abbaspour, M.A.A. Sadatlu, S. Mirkiani, A. Ghasemi, M. Hoseini-Ghahfarokhi, N. Mozaffari, M. Karimi, and M.R. Hamblin, ChemistrySelect **5**, 10200 (2020).
12. Y. Chen, P. Pötschke, J. Pionteck, B. Voit, and H. Qi, Journal of Materials Chemistry A **6**, 7777 (2018).
13. Y. Pang, J. Yang, T.E. Curtis, S. Luo, D. Huang, Z. Feng, J.O. Morales-Ferreiro, P. Sapkota, F. Lei, J. Zhang, Q. Zhang, E. Lee, Y. Huang, R. Guo, S. Ptasinska, R.K. Roeder, and T. Luo, ACS Nano **13**, 1097 (2019).
14. T.V. Pham, J. Kim, J.Y. Jung, J.H. Kim, H. Cho, T.H. Seo, H. Lee, N.D. Kim, and M.J. Kim, Advanced Functional Materials **29**, 1905511 (2019).
15. M. Son, S.-S. Chee, S.-Y. Kim, W. Lee, Y.H. Kim, B.-Y. Oh, J.Y. Hwang, B.H. Lee, and M.-H. Ham, Carbon N Y **159**, 579 (2020).
16. J. Wang, M. Kim, L. Chen, K.-M. Ho, M. Tringides, C.-Z. Wang, and S. Wang, Physical Review B **103**, 085403 (2021).
17. H. Muramatsu, Y.A. Kim, K.-S. Yang, R. Cruz-Silva, I. Toda, T. Yamada, M. Terrones, M. Endo, T. Hayashi, and H. Saitoh, Small **10**, 2766 (2014).
18. R. Ikram, B.M. Jan, and W. Ahmad, Journal of Materials Research and Technology **9**, 15924 (2020).
19. P. Singh, J. Bahadur, and K. Pal, Graphene **06**, 61 (2017).
20. I. Rhee, Y.A. Kim, G.-O. Shin, J.H. Kim, and H. Muramatsu, Construction and Building Materials **96**, 189 (2015).
21. F.E. Che Othman, M.S. Ismail, N. Yusof, S. Samitsu, M.Z. Yusop, N.F. Tajul Arifin, N.H. Alias, J. Jaafar, F. Aziz, W.N. Wan Salleh, and A.F. Ismail, Carbon Letters **30**, 535 (2020).
22. M.S. Ismail, N. Yusof, M.Z. Mohd Yusop, A.F. Ismail, J. Jaafar, F. Aziz, and Z. Abdul Karim, Malaysian Journal of Fundamental and Applied Sciences **15**, 516 (2019).
23. M.A. Seitzhanova, Z.A. Mansurov, M. Yeleuov, V. Roviello, and R. di Capua, Eurasian Chemico-Technological Journal **21**, 149 (2019).
24. S. Sankar, H. Lee, H. Jung, A. Kim, A.T.A. Ahmed, A.I. Inamdar, H. Kim, S. Lee, H. Im, and D. Young Kim, New Journal of Chemistry **41**, 13792 (2017).
25. N.F. Tajul Arifin, N. Yusof, N.A.H. Md Nordin, J. Jaafar, A.F. Ismail, F. Aziz, and W.N. Wan Salleh, International Journal of Hydrogen Energy **46**, 31084 (2021).
26. O.F. Abraham, V.S. Aigbodion, E.C. Ejiogu, and U.C. Ogbuefi, Diamond and Related Materials **123**, 108885 (2022).

27. M. Seitzhanova, D. Chenchik, M. Yeleuov, Z. Mansurov, R. di Capua, and N. Elibaeva, Chemical Bulletin of Kazakh National University **89**, 12 (2018).
28. Y. Liu, J. Chen, B. Cui, P. Yin, and C. Zhang, C (Basel) **4**, 53 (2018).
29. B. Li and K. Li, Chemosphere **220**, 28 (2019).
30. C. Wang, R. Zou, M. Qian, X. Kong, E. Huo, X. Lin, L. Wang, X. Zhang, R. Ruan, and H. Lei, Bioresource Technology **355**, 127251 (2022).
31. J.C. Solarte-Toro, J.M. Romero-García, J.C. Martínez-Patiño, E. Ruiz-Ramos, E. Castro-Galiano, and C.A. Cardona-Alzate, Renewable and Sustainable Energy Reviews **107**, 587 (2019).
32. A.T. Hoang, S. Nizetic, H.C. Ong, C.T. Chong, A.E. Atabani, and V.V. Pham, Journal of Environmental Management **296**, 113194 (2021).
33. S. Deng and V. Berry, Materials Today **19**, 197 (2016).
34. M.N. Esfahani, M. Jabbari, Y. Xu, and C. Soutis, Materials Today Communications **26**, 101856 (2021).
35. L. Fan, J. Xu, and Y. Hong, RSC Advances **12**, 6772 (2022).
36. H. Guo and J. Wang, Nanomaterials **12**, 764 (2022).
37. N.F.T. Arifin, N. Yusof, N.A.H.M. Nordin, J. Jaafar, A.F. Ismail, F. Aziz, and W.N.W. Salleh, IOP Conference Series: Materials Science and Engineering **991**, 012112 (2020).
38. S.K. Sharma, G. Sharma, A. Sharma, K. Bhardwaj, Km. Preeti, K. Singh, A. Kumar, V.K. Pal, E.H. Choi, S.P. Singh, and N.K. Kaushik, Applied Surface Science Advances **8**, 100225 (2022).